RSC Advances

PAPER

View Article Online
View Journal | View Issue

Cite this: *RSC Adv.*, 2020, **10**, 5930

Visible light driven photo-reduction of Cu^{2+} to Cu_2O to Cu in water for photocatalytic hydrogen production†

Shuang Cao,‡[ab] Chuan-Jun Wang,‡*[c] Guo-Qiang Wang,[c] Yong Chen,[ab] Xiao-Jun Lv[ab] and Wen-Fu Fu*[abd]

Metal nanoparticles are synthesized *via* various methods and have found many applications in areas such as sensing, electronics and catalysis. Light induced formation of noble metal nanoparticles, especially platinum, in solution or loaded on semiconductor surfaces, is an established practice in photocatalysis. Nevertheless, preparation of catalytically-active non-precious metal nanoparticles *via* photo-reduction still have room to be further explored. Here, we report a visible light driven system that can coordinate photo-reduction of $CuSO_4$ to selectively prepare Cu_2O or Cu nanoparticles, while at the same time, mediating efficient hydrogen production with *in situ* generating Cu catalyst without further need to add any components. The Cu_2O and Cu nanoparticles *in situ* generated are crystalline in nature and can perform as pre-catalyst (Cu_2O) or catalyst (Cu) to catalyze hydrogen production when reincorporated into the same photo-reduction system with organic photosensitizers. Our work offers an exploratory pathway to prepare target metal nanoparticles while provides some insight into harnessing solar energy for multi-functional purposes.

Received 19th November 2019
Accepted 24th January 2020

DOI: 10.1039/c9ra09590j

rsc.li/rsc-advances

Introduction

The worldwide fossil-fuel-depletion propels urgent quests for alternative solutions regarding renewable energy resource supplies. Solar energy provides our planet with a vast amount of energy that possess great potential to solve energy problems. Major approaches concerning utilization and conversion of solar energy like the photosynthesis of green plants in nature and the solar cells for electricity generation are versatile but also are limited.[1] Developing means of artificial photosynthesis for effectively harnessing solar energy is crucial for the sustainable development of human society.[2–5] Photocatalytic hydrogen production has been regarded as a promising solution to relieve the crisis triggered by depletion of fossil fuels.[6] Multi-component systems with metal complex mimics as light sensitizer or catalyst have been extensively explored during the past few decades.[6–9] Many research studies in this area concern the development of non-precious metal based molecular catalysts to replace noble metal Pt nanoparticles for efficient hydrogen production.[10–17] Pt is rare and expensive, which limits its general application. A substantial amount of active molecular photocatalysts based on active metal centers like Fe,[8,18] Co,[10] Ni[8,11–13] have been developed. However, one side effect for most homogeneous molecular catalysts is their degradation when either light intensity or irradiation time is increased.[18] Heterogeneous nanoparticle catalysts possess advantages such as easy preparation, good stability, excellent recyclability and reusability. The development of hybrid systems where metal nanoparticles could act as efficient photocatalysts with organic photosensitizers could combine the versatility of homogeneous catalysis with the advantages of heterogeneous catalysts. Copper, one of the most widely used metal in human society, has received increasing attention in photocatalytic hydrogen production. For instance, there have been previous reports on Cu loaded on semiconductors for water reduction under light irradiation.[19–23] Copper based molecular catalysts are rare, and there have been literature reported the pre-synthesis of PVP stabilized Cu nanoparticles with 2-phenyl-4-(1-naphthyl) quinolinium as photosensitizer and NADH as sacrificial electron donor in organic water mixed solution under acidic conditions for water reduction, but the hydrogen evolution efficiency is low compared with Ni nanoparticles.[24] To make further contribution in this area of study, it is highly desirable to explore systems where stable Cu nanoparticles can combine

[a]*Key Laboratory of Photochemical Conversion and Optoelectronic Materials, CAS-HKU Joint Laboratory on New Materials, Technical Institute of Physics and Chemistry, Chinese Academy of Sciences, Beijing 100190, P. R. China. E-mail: fuwf@mail.ipc.ac.cn*

[b]*University of Chinese Academy of Sciences, Beijing 100049, P. R. China*

[c]*College of Chemistry and Material Science, Shandong Agricultural University, Tai'an 271018, P. R. China. E-mail: wangchuanjun@sdau.edu.cn*

[d]*College of Chemistry and Engineering, Yunnan Normal University, Kunming 650092, P. R. China*

† Electronic supplementary information (ESI) available. See DOI: 10.1039/c9ra09590j

‡ The authors have contributed equally to this work.

with cheap organic sensitizers for water reduction in pure neutral or alkaline water solution. The research would hold prospect for coupling to water oxidation reaction, which is thermodynamically possible in basic solution.

On the other hand, preparation of metal or metal oxide nanoparticles is crucial for the subsequent use in catalysis. Currently, it has been mostly conducted *via* chemical methods[25] with thermal decomposition, phase-transfer method, use of ionic liquids and microwave synthesis. Some of these processes require coating of the nanoparticles with stabilizing agent, which is often unfavorable for catalytic reactions to take place on active metal surface sites.[26,27] Light induced *in situ* generation of nanoparticles from metal salt precursors holds significance in water splitting reactions.[28–32] There have been reports on photo-generation of Cu in $Cu(OH)_2/TiO_2$ (ref. 33) and Cu_2O/TiO_2 (ref. 34) photocatalysts under UV light irradiation. But as far as we know, there has been few work on photo-generation of Cu based nanoparticles in a homogeneous system incorporating organic dyes as reduction agent and photosensitizer, the investigation of such systems may provide further details of mechanistic insight.

In this work, we demonstrate a bi-functional visible light driven system incorporating fluorescein as photosensitizer and reducing agent, and $CuSO_4$ salt as precursor in alkaline TEA or TEOA aqueous solution, for photo-generation of Cu_2O and Cu nanoparticles and simultaneous photocatalytic hydrogen production. Tunable preparation of Cu_2O or Cu particles is realized by adjusting the choice of TEA and TEOA sacrificial electron donors and exerting control over photo-irradiation time. A stepwise light driven photochemical process from $Cu(OH)_2$ to Cu_2O to Cu, which was the real photocatalyst, was proposed based on real-time X-ray diffraction (XRD) monitoring and corroborated hydrogen production experiments. When the *in situ* generated Cu_2O and Cu were incorporated into the same photocatalytic system in place of $CuSO_4$, robust hydrogen production were observed, the system lasted for more than 140 hours with no significant decrease in efficiency and large amounts of hydrogen evolved. A single crystal of a $Cu(TEOA)(H_2O)_2$ complex was also cultivated and analyzed, together with a series of dynamic light scattering (DLS), XRD and induction period measurements, it greatly contributes to the clarification of mechanism. It is intriguing that by incorporating Fl and $CuSO_4$ in an alkaline TEOA or TEA solution, and presiding control over photo-irradiation time, we have successfully acquired Cu_2O and Cu nanocrystals while simultaneously achieved hydrogen evolution in one system. Our work is expected to provide some new insight on harnessing solar energy for applications in photocatalysis.

Experimental

Assembly of photocatalytic system and hydrogen measurement

In a typical reaction, Fl (10^{-3} M) was added into a 60 mL quartz tube containing $CuSO_4 \cdot 5H_2O$ (1.0×10^{-5} M) and TEA or TEOA (5%, v/v) aqueous solution (30 mL) at pH 11 or 10 (adjusted with 0.1 M HCl). The solution was deoxygenized with N_2 for 30 minutes and then the tube was sealed with a rubber cap. The 10 samples (10 tubes containing the same components for parallel experiment) were subjected to irradiation apparatus comprising LED light source (30×3 W, $\lambda > 420$ nm) and magnetic stirrer. The focused intensity on the flask was about 16 mW cm^{-2}. The number of incident photons was 3.35×10^{17} photons per s as measured by using an irradiance meter. The generated hydrogen from the systems was measured at different time intervals by GC-14C (Shimadzu) which was equipped with a 5 Å molecular sieve column (3 m $\times$ 2 mm), thermal conductivity detector and N_2 carrier gas. The amount of hydrogen was quantified by an external standard method. The turnovers were calculated based on the mole amount of added $CuSO_4$.

Characterization methods

The prepared Cu_2O and Cu nanoparticles collected at different time intervals was washed several times with deoxygenated ethanol, centrifuged and dried under an inert atmosphere. The dried nanoparticles were directly used for XRD measurement. For TEM measurement, the nanoparticles were dispersed in deoxygenated ethanol solution. High-resolution transmission electron microscopy (HRTEM) was performed on JEM 2100F which is operated at an accelerating voltage of 200 kV. The SEM images were taken on a Hitachi S-4800 field emission scanning electron microscope operating at 5.0 kV. SEM samples were prepared by drop-casting suspensions onto silicon wafers. X-ray powder diffraction (XRD) spectra were collected on a Bruker D8 Focus under Cu-Kα radiation at ($\lambda = 1.54056$ Å). The pH values were adjusted with a Model pH S-3C meter (Mettler Toledo FE20). Dynamic light scattering (DLS) measurements were performed with a Dynapro NanoStar instrument (Wyatt Technology). The DLS instrument used in this study can detect particle sizes ranging from 0.5 to 2000 nm. The light source for the scattering experiments is a He–Ne gas laser (100 mW, $\lambda =$ 658 nm). Data were obtained using a scattering angle of 90° at 25 °C.

Results and discussion

Hydrogen production and tunable preparation of nanoparticles

The photocatalytic system was assembled by adding a certain amount of catalyst precursor $CuSO_4$ (10^{-4} M) into 30 mL 5% TEA or TEOA sacrificial electron donor aqueous solution, fluorescein (1 mM) was introduced as light sensitizer and reduction agent. Under visible light irradiation, synchronous production of nanoparticles and hydrogen could be observed and determined. Moreover, control experiments showed that when either light irradiation is absent or any component is missing from the system, neither particle formation nor any significant amount of hydrogen evolution can be detected. Optimization of photocatalytic parameters includes different sacrificial donors, pH, photosensitizers, the concentration of Fl and precursor Cu^{2+} ions.

A screen of sacrificial reagents used, from TEA, TEOA to methanol to acetic acid and ascorbic acid revealed that only in

the presence of basic TEA and TEOA, can the photocatalytic system show photo-reduction and hydrogen evolution activity. The fact that ascorbic acid, a common effective electron donor[13,16] with smaller oxidation potential and is more easily oxidized,[35] renders as ineffective sacrificial agent, indicates the strong influence of pH value on the photocatalytic activity of the system. The reason the system is functional in alkaline solution could be associated with the formation of $Cu(OH)_2$ pre-catalyst, fulfilling the photo-reduction process of $Cu(OH)_2$ to Cu_2O (-0.08 V *vs.* NHE) and Cu_2O to Cu (-0.358 V *vs.* NHE). This supposition is in accordance with the photocatalytic phenomenon and will be further discussed in mechanistic part. pH often has strong influence on the excited states of photocatalytic components.[12] The influence of pH values on H_2 production is scrutinized, the rate of H_2 production is highest at pH 11 and 10 in TEA and TEOA solutions respectively (ESI Fig. S1 and S2†). A scrutiny of the photosensitizers used in TEOA and TEA systems revealed that Fl is the most effective one compared with other rhodamine dyes like Erythrosin B, Eosin Yellowish and Rose Bengal (ESI Fig. S3 and S4†). In addition, the concentration of Fl was also tested, the highest hydrogen production activity in TEOA and TEA solutions were found with Fl concentration of 1 mM (ESI Fig. S5 and S6†). At low concentrations of Fl (0.2, 0.5 mM) the system quickly lost hydrogen evolution activity within 12 hours of light irradiation due to the bleach of sensitizers to generate excited states. However, hydrogen production rates are also low at high Fl concentrations, (0.2, 0.5 mM) which may be ascribed to the inefficient input of light and self-quenching of excited state molecules caused by aggregation of dyes in high concentration.[36]

When varying $CuSO_4$ concentrations for hydrogen production, interesting experimental phenomenons were observed which are crucial to the selective preparation of Cu_2O and Cu nanoparticles. The influence of Cu^{2+} concentration was examined with Fl (1.0×10^{-3} M) and in 30 mL 5% TEA or TEOA aqueous solution adjusted to the optimized pH value (Fig. 1a and b).

In the TEA system, the hydrogen production rate enhanced dramatically with increasing amounts of added $CuSO_4$. At 10^{-3} M Cu^{2+} concentration, particle formation was quickly observable to eye upon light irradiation and 4.6 mL H_2 was generated within 4 hours of irradiation, corresponding to an initial rate of 1.15 mL h^{-1}. However, the system had shorter lifetime at higher Cu^{2+} concentration, which is probably due to the fast consummation of Fl and TEA for photo-reduction of particles and photo-evolution of hydrogen. At 10^{-6} M, the hydrogen production system was low in efficiency but with longer lifetimes, hydrogen production was almost linear for the first 10 hours of irradiation with a turnover frequency (TOF) value of 173 h^{-1} and a turnover number of 2633 was achieved based on added $CuSO_4$ concentration after 22 hours of irradiation. By contrast, the TEOA system exhibited different experimental results. The initial hydrogen production rate was low but the system displayed longer lifetime compared with those in TEA solution. For instance, at 10^{-4} M Cu^{2+} concentration, hydrogen production rate of the first 6 hours is only 0.45 mL h^{-1} with TEOA compared with 0.71 mL h^{-1} with TEA as sacrificial reagent, but hydrogen evolution was almost linear for an irradiation period of 25 hours in TEOA aqueous solution, but ceased activity within 12 hours of illumination in TEA system. The improvement in hydrogen evolution rate was also observed in TEOA solution with increasing of Cu^{2+} from 10^{-6} M to 10^{-4} M. However, when the catalyst precursor concentration was further increased to 10^{-3} M, no hydrogen evolution activity was detected for the first 30 min of light irradiation and hydrogen evolution rate was all the way lower than when Cu^{2+} concentration was 10^{-4} M.

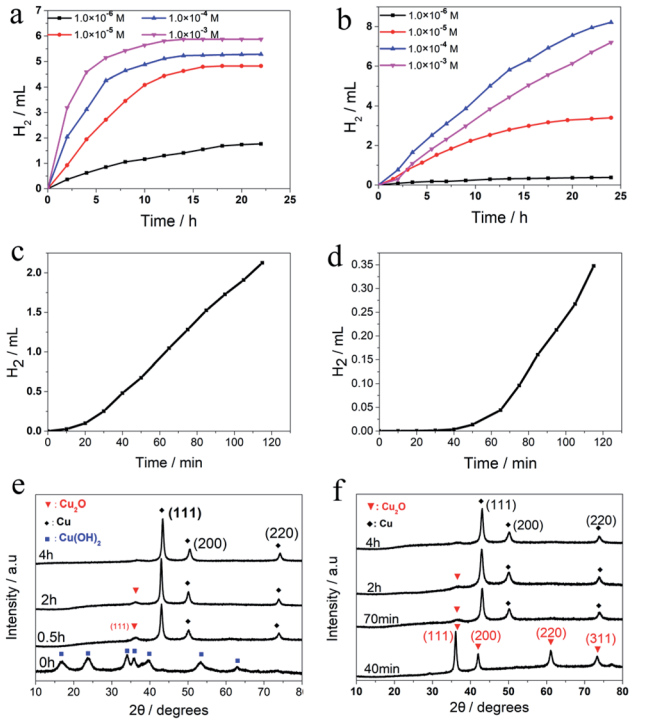

Fig. 1 Time course of H_2 evolution from systems containing Fl (1.0 mM) and (5% v/v) TEA (a) or TEOA (b) in 30 mL H_2O at pH 11 (a) or 10 (b) in a 60 mL volume quartz tube upon irradiation with $\lambda > 420$ nm LED light with various concentrations of $CuSO_4 \cdot 5H_2O$. Induction period experiments of H_2 evolution in the first 2 hours from system containing Fl (1.0 mM), Cu^{2+} (1.0×10^{-3} M) in (5% v/v) TEA (c) or TEOA (d) aqueous solution at optimized pH values. (e) XRD patterns of the precipitates collected at different irradiation time from a system have the same experimental conditions as (c). (f) XRD patterns of the precipitates collected at different irradiation time from a system have the same experimental conditions as (d).

Accordingly, we performed some induction-period-measurements together with real-irradiation-time XRD experiments to shed light on the situation. Induction period experiments with Cu^{2+} concentration of 10^{-3} M in 5% TEOA and TEA solution was conducted (Fig. 1c and d). It revealed that no hydrogen evolution occurred within the first 40 min in TEOA solution, but for system with TEA, hydrogen evolution happens after 10 min of light irradiation. On examination of the photocatalytic solution, we observed the solution become turbid with particles. Therefore, the precipitates at different irradiation times were collected and characterized by XRD measurements to clarify the reason behind the different hydrogen production results in TEOA and TEA solution, and to identify the changes of added Cu^{2+} going through during photocatalytic process. For the TEA system,

blue precipitate was immediately formed when $CuSO_4$ (10^{-3} M) was added into the basic TEA aqueous solution. From the XRD patterns (Fig. 1e), characteristic diffraction peaks of $Cu(OH)_2$ were observed. There were six main diffraction peaks near or at $2\theta =$ 16.7, 23.8, 34.1, 35.9, 39.8, 53.2 and 63.2°, corresponding to (020), (021), (002), (111), (130), (150) and (043) diffraction planes of $Cu(OH)_2$ (JCPDS 12-420),[31] respectively. After 30 minutes irradiation, black particles were obtained and proved to be mainly Cu(0), with the reflection peaks corresponding to the Cu diffraction plane of (111), (200) and (220).[37] At the same time, only a small amount of Cu_2O was also detected with the diffraction plane of (111).[38] Under the same experimental conditions, particles collected after 2 h of irradiation exhibited the similar XRD patterns with that irradiated for 30 minutes, but with decrease in intensity for Cu_2O (111) reflection peak, indicating a further diminish in Cu_2O amount. Samples tested after 4 h of light illumination displayed only the Cu(0) reflection peaks and a complete absence of Cu_2O. Collectively, these XRD measurements provide us with three items of important information. First, XRD measurements at different hours revealed a fast photochemical process from $Cu(OH)_2$ to Cu_2O and Cu, and the gradual transformation of Cu_2O to Cu under visible light irradiation in the TEA solution. Second, when coordinating these XRD data with hydrogen production results (Fig. 1a and c), we can identify Cu(0) as an effective photocatalyst and $Cu(OH)_2$ is not. As in the first five minutes when the system is overall with the presence of $Cu(OH)_2$, but no hydrogen is detected and hydrogen evolution is low within the first 20 minutes. In addition, the fact that Cu_2O was fully transformed into Cu(0) after 4 h of irradiation while hydrogen production was active for more than 10 hours, is proof that Cu(0) can act as effective catalyst. Third, we have made clear the irradiation time necessary for the selective preparation of pure Cu nanoparticles in the TEA system is irradiation after 4 hours.

For the TEOA system, when Cu^{2+} (10^{-3} M) was added into the solution, no precipitation but an indigo blue clear solution was observed. Single crystals were cultivated and we found $Cu(TEOA)(H_2O)_2$ complex was formed in the solution based on X-ray single crystal diffraction method. However, the clear solution quickly turned turbid upon light irradiation. As irradiation for 40 min produced no H_2 (Fig. 1d), the particles formed at 40 min were collected and were found to be dark red in color. XRD measurement showed that these nanoparticles were pure Cu_2O in form (Fig. 1f).[35] However, samples measured at 70 min showed that Cu(0) is predominant in these particles. A further diminish in Cu_2O amount is observed for samples irradiated 2 h, and complete transformation of Cu_2O to Cu was also observed for samples measured after 4 h of irradiation (Fig. 1f). Three important pieces of information can also be extracted from these experiments. First, $Cu(TEOA)(H_2O)_2$ complex is not photocatalyst for hydrogen production in our system. As no hydrogen production activity is observed in the first 40 min of irradiation (Fig. 1d). Second, Cu is the sole efficient catalyst for hydrogen evolution in our system. There has been previous report of using Cu_2O for overall water splitting under visible light irradiation with a comparatively large amount of Cu_2O under prolonged irradiation time (1900 h). The amount of Cu^{2+} within our system is much less (10^{-3} M), irradiation of the system for 40 min produced pure Cu_2O but no accountable amount H_2 proved that Cu_2O is not an active photocatalyst to accept excited state electrons from Fl for hydrogen evolution. Only when Cu was generated, can efficient hydrogen evolution occur. Third, by adopting TEOA as the sacrificial agent and exerting precise control over the irradiation time, we have successfully realized the tunable-phase selective preparation of pure Cu_2O and Cu nanoparticles in one photocatalytic system while at the same time achieved substantial hydrogen evolution. In addition, when the concentration of Cu^{2+} is lowered, although evolution of hydrogen could be detected earlier, it was difficult to collect the precipitate for XRD measurement as the few particles *in situ* generated were well dispersed in the solution. However, we could perorate that Cu^{2+} was reduced to Cu_2O and then to Cu(0) as in 1 mM Cu^{2+} concentration systems. Lower the concentration of Cu^{2+} would result in faster photo-reduction processes from Cu^{2+} to Cu_2O to Cu(0), and therefore the earlier evolution of hydrogen gas.

Characterization of Cu_2O and Cu nanoparticles

The identity of the tunably prepared Cu_2O and Cu nanoparticles was initially characterized by XRD methods. We then utilized a couple of other techniques to acquire more information regarding the morphology and nano-scale interaction of these *in situ* generated particles, which we hope will provide some mechanistic insights regarding the photocatalytic process. The isolated Cu_2O and Cu nanoparticles were examined by transmission electron microscopy (TEM) and scanning electron microscopy (SEM) (Fig. 2). It was found that most of the Cu_2O (Fig. 2a and b) and Cu (Fig. 2d and e) particles were spherical in form and the majority of them were in the state of agglomeration. Some of the Cu_2O nanoparticles are 200 nm to 600 nm in size (Fig. 2a), HRTEM image of their edges showed that these particles were composed of numerous tiny highly crystalline nanoparticles with the size around 2–5 nm (Fig. 2a, inset). The selected area electron diffraction (SAED) pattern showed that both the Cu_2O (Fig. 2d inset) and Cu (Fig. 2e inset) nanoparticles had diffraction rings of single crystal. The nanoparticles were found to have good crystalline behaviour, with clear single crystal lattices observed. The spacing of 0.21 nm between adjacent lattice planes was measured for Cu_2O, which corresponds to the distance between two (200) crystal planes of Cu_2O (Fig. 2d).[38] Lattice crystal plane spacing of 0.208 nm was also measured for Cu nanoparticles and can be ascribed to the diffraction of (111) Cu planes.[37] In addition, the XPS results were also conducted on Cu nanoparticles collected after 4 h of irradiation in both systems, and on Cu_2O nanoparticles collected after 40 min of irradiation in TEOA system. The results showed that compared to that of Cu, The Cu $2p_{2/3}$ and Cu $2p_{1/2}$ peaks of Cu_2O shifted to lower binding energy. The same trend was reported in previous literature (Fig. S7†).[20]

Robust hydrogen production with isolated Cu_2O and Cu nanoparticles

The tunably prepared Cu_2O and Cu nanoparticles were reincorporated into the photocatalytic system as precatalyst or

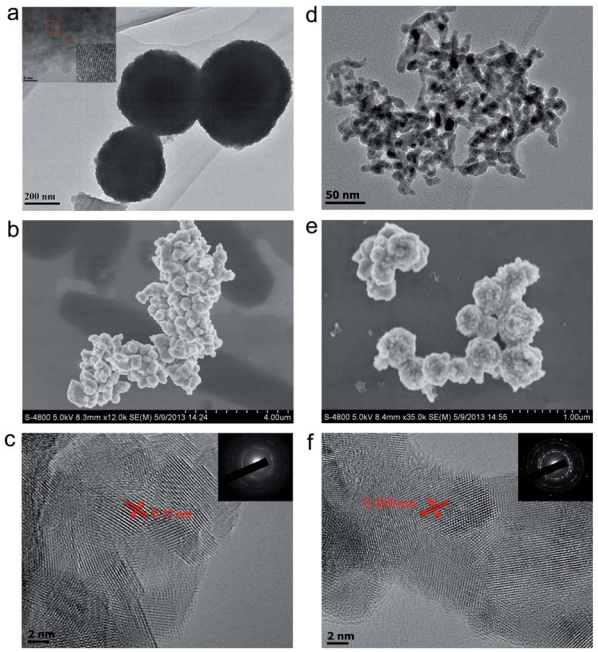

Fig. 2 TEM (a), SEM (b) and HR-TEM (c) images of the tunably prepared Cu_2O nanoparticles. TEM (d), SEM (e) and HR-TEM (f) images of the Cu nanoparticles formed *in situ* under visible light irradiation. Inset of (a): HRTEM image of the edges of the nanoparticles.

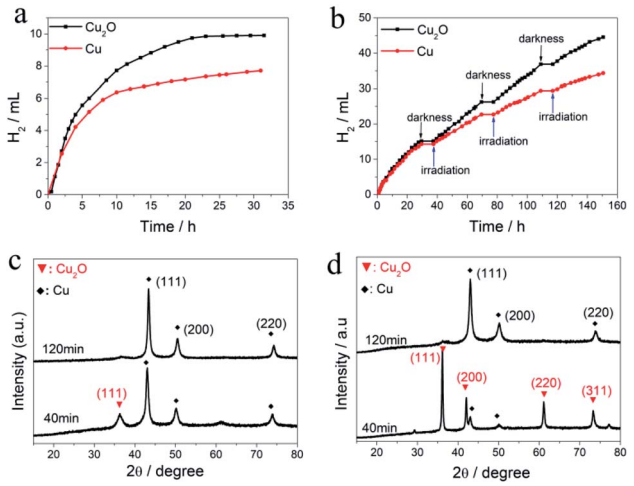

Fig. 3 Hydrogen production from systems incorporating *in situ* generated Cu_2O (black line) (30 μM, 4.4 mg) or Cu (red line) nanoparticles (30 μM, 2 mg) with Fl (2.0 mM) in 30 mL (5% v/v) pH = 11 TEA (a) or (5% v/v) pH = 10 TEOA (b) aqueous solution. (c) and (d) XRD patterns measured at different irradiation times. Sample precipitates were collected from systems initially containing Cu_2O nanoparticles (30 μM, 4.4 mg) with Fl (2.0 mM) in 30 mL pH = 11 (5% v/v) TEA (c) or 30 mL pH = 10 (5% v/v) TEOA (d) aqueous solution.

catalyst for photocatalytic hydrogen evolution. When Cu_2O (30 μM, 4.4 mg) or Cu (30 μM, 2 mg) was added into systems containing 2 mM Fl photosensitizer in 30 mL 5% TEA or 5% TEOA aqueous solution (Fig. 3c and d), different experimental results were obtained. In the first place, for systems incorporating Cu(0) nanoparticles, instantaneous evolution of hydrogen could be detected upon visible light irradiation. The *in situ* generated Cu(0) could perform as stable and robust photocatalyst for hydrogen production in the alkaline aqueous solution. For system incorporating TEA as sacrificial electron donor, a total amount of 7.7 mL H_2 could be obtained after 31 hours of irradiation (Fig. 3a); for systems with TEOA as sacrificial agent, the system exhibited extraordinarily stable activity, photocatalytic reaction steadily went on for more than 140 h with no significant decrease in hydrogen production rate, producing 35 mL H_2 in a single run without extra adding of components (Fig. 3b). In the second place, when Cu_2O pre-catalyst was added into the systems, hydrogen production was found to experience an induction period (Fig. S8 and S9†), due to the photo-reduction of Cu_2O to Cu(0) photocatalyst (Fig. 3c–f). In TEA solution, the induction period was found to be short with hydrogen evolution happened after 10 min of irradiation (Fig. S8†), and hydrogen production continued for more than 20 h, with more than 9.7 mL hydrogen generated (Fig. 3a). In contrast, the induction period took almost 40 min before hydrogen evolution occurred in TEOA solution (Fig. S9†). Similar as when using Cu as photocatalyst, hydrogen production was more robust in TEOA solution, with more than 44 mL H_2 produced after about 140 h of photocatalytic reaction (Fig. 3b). Previous reports showed that TEOA could prevent back-reaction between PS^+ and PS^- and stabilize the radicals, thereby prolonging the lifetime of singlet excited state of PS. On the contrary, a higher concentration of TEA led to decrease in photocatalytic efficiency because of back-reaction between Fl* and TEA^+.[39–41] Therefore, the sharp decrease of activity after 20 h in TEA was due to the consumption of Fl. In the third place, we again employed XRD methods to shed light on the time-course transformation of Cu_2O to Cu in the photocatalytic system with either TEA or TEOA sacrificial agents (Fig. 3c and d). Most of the Cu_2O was found to be transformed into Cu(0) after 40 min of light irradiation in TEA solution while in TEOA solution only trace amounts of Cu(0) was generated at that time. In accordance with XRD measurements in Fig. 1, these results proved that Cu(0) is the active catalyst in our system and also demonstrated a faster photo-reduction rate of Cu_2O to Cu when TEA was adopted as the sacrificial electron donor. In the fourth place, we found that for both Cu_2O and Cu incorporated, when use TEA as sacrificial agent, the system had a higher H_2 evolution rate than when TEOA was used before 10 h of irradiation (Fig. S10 and S11†). After 10 h, hydrogen evolution of both Cu_2O and Cu in TEA experienced sharp decrease in efficiency and nearly lost activity after 20 h (Fig. S10†). However, hydrogen evolution of Cu_2O and Cu in TEOA increased almost linearly even after 10 hours of irradiation and continually produced hydrogen for more than 120 hours (Fig. S10†). In the last place, hydrogen evolution rate with Cu_2O (30 μM, 4.4 mg) was lower than with Cu (30 μM, 2 mg) in the first few hours, which is due to the lower amount of Cu catalyst in the system during the Cu_2O transformation process (Fig. 3a and b). However, for systems incorporate Cu_2O (30 μM, 4.4 mg), hydrogen production surpassed both in rate and amount after a few hours of irradiation. This can be attributed to the completion of induction period and

fully transformation of Cu_2O (30 μM, 4.4 mg) to Cu catalyst (theoretically 60 μM, 3.9 mg), which has a larger value than systems with added Cu (30 μM, 4.4 mg). In short, we have proved that the *in situ* generated Cu_2O and Cu nanoparticles could serve as effective pre-catalyst or catalyst for photocatalytic hydrogen production when incorporated into the same system containing Fl and TEA or TEOA. Transformation of Cu_2O to Cu, which is the real efficient catalyst in our system, was established and the high photocatalytic activity may be in part attributed to the active facets of the highly crystalline nanoparticles.

Furthermore, as can be seen from the microscopic images (Fig. 2), the generated Cu nanoparticles showed agglomerated behaviour, which self-assembly into larger nanoparticles. To improve the catalytic efficiency, it is highly necessary to adopt methods that can prevent the overgrowth of nanoparticles,[42] such as carbon layer protection,[43] introducing graphene as support to form composite material,[30,31] use of growth directing agents[44] *et al.* In a following work, we managed to prepare dendritic copper based nanoparticles with uniform size around 20 nm in a photocatalytic system with PVP as directing agent, which we would hopefully to demonstrate in further work.

Mechanistic insights

The photochemical processes governing the photo-reduction of Cu^{2+} in solution is further investigated to provide some mechanistic insights into the time-coursed *in situ* phase formation of Cu_2O and Cu nanoparticles and the disparity of hydrogen evolution in TEOA or TEA aqueous solution (Fig. 4). As we have discussed above, when $CuSO_4$ (10^{-3} M) was added into TEA solution, instantaneous formation of blue precipitate was observed and prove to be $Cu(OH)_2$ by XRD measurements (Fig. 1e). Subsequent fast transformation of $Cu(OH)_2$ to Cu_2O and then to Cu was happening within 10 minutes and was also monitored by real-time XRD experiments (Fig. 1e and 3c). Bernhard's group reported the photo-reduction of Zn^{2+} to Zn metal with molecular Ir complex as photosensitizer and TEA as electron donor under visible light irradiation.[45] For our system, excited state Fl* and Fl^- generated upon light irradiation have reduction potentials of −1.7 and −1.3 V,[12] which possess sufficient driving force to provide electrons for reduction of $Cu(OH)_2 \rightarrow Cu_2O$ (−0.08 V *vs.* NHE) and $Cu_2O \rightarrow Cu$ (−0.358 V *vs.* NHE). Upon generation of Cu, the excited state fluorescein further provide electrons to Cu(0) for photocatalytic hydrogen production. As has been discussed in literature,[31] when the concentration of TEA is high (5% v/v) in the system, the excited state Fl* would be first quenched by TEA through a reductive quenching mechanism to form Fl^-, which then transfers electron to the precatalyst for reduction process. Therefore, we may safely conclude that the photochemical process in TEA solution is the photo-induced electron transfer from Fl* to $Cu(OH)_2$ through reductive quenching process.

In TEOA solution, however, no sign of the formation of $Cu(OH)_2$ was observed but an indigo blue clear solution when $CuSO_4$ was added. It is reasonable to assume that Cu^{2+} would coordinate with TEOA to form molecular complex which is soluble in the solution as previously reported for Ni^{2+} and TEOA.[46] Fortunately, single crystals were cultivated by adding $CuSO_4$ in aqueous solution in the presence of excess TEOA, the crystal structure determined by X-ray single crystal method revealed the structure of a $Cu(TEOA)(H_2O)_2$ complex, with all of the three O and N atoms of one TEOA molecule plus two water molecules coordinated to Cu^{2+} (Fig. S12†). On the other hand, we have already proved that this $Cu(TEOA)(H_2O)_2$ complex is not a molecular catalyst for hydrogen production through a series of hydrogen production induction-period and XRD experiments (Fig. 1d and f). During photocatalytic experiments, the system quickly turned turbid upon light irradiation for a few minutes, continually producing Cu_2O within the first 40 minutes of irradiation. Only when Cu nanoparticles were generated after 40 min could evolution of hydrogen occur (Fig. 1d and f). Therefore, it is likely that the same photochemical process from $Cu(OH)_2$ to Cu_2O to Cu catalyst was happening in TEOA solution.

For systems incorporating TEOA sacrificial donor, the pH of the solution optimized for hydrogen evolution is at pH = 10 (Fig. S2†), fast formation of turbids in the solution upon light irradiation means that the $Cu(TEOA)(H_2O)_2$ complex was unstable and could dissociate Cu^{2+} upon light irradiation, which would coordinate with OH^- in the alkaline condition to form $Cu(OH)_2$ precatalyst to undergo transformation to Cu_2O and Cu. To support this supposition, dynamic light scattering experiments were employed to supply additional evidence (Fig. S13†). Before light irradiation, some particles with the size around 200 nm were detected in the photocatalytic system (Fig. S13a†), which indicates the presence of $Cu(OH)_2$ nanoparticles in the system. Photo-irradiation of the TEOA system for 4 min saw the emergence of particles (Fig. S13c†) around 1500 nm in size, which amount increased after 7 min of irradiation (Fig. S13d†). The size of the particles generated corresponds to the Cu_2O size in the SEM images (Fig. 2b) and proves the photo-reduction process from $Cu(OH)_2$ to Cu. So formation of $Cu(TEOA)(H_2O)_2$ complex in TEOA solution has the effect of controlled-release of Cu^{2+} to continually form $Cu(OH)_2$ precatalyst for slow transformation to Cu_2O and then to Cu. This proposition is in accordance with the longer induction period

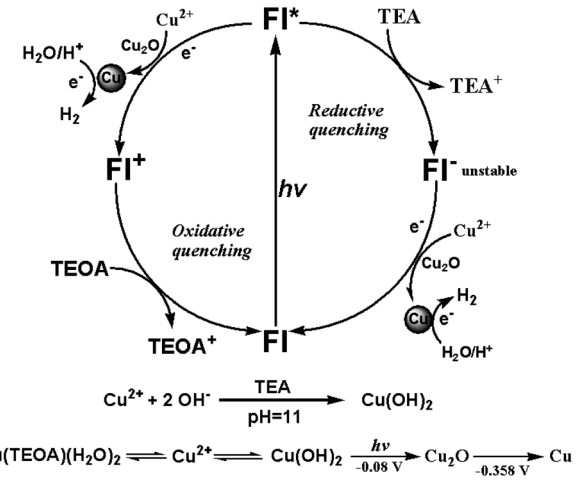

Fig. 4 Schematic illustration of the photocatalytic process.

measured for hydrogen production in TEOA system. As for the longer induction period observed for TEOA system directly incorporating Cu_2O as precatalyst, we may also find root in the unique structural property of TEOA with its three coordinating oxygen atoms, which upon dissociation with Cu^{2+} may have the ability to readily enclose the *in situ* generated Cu_2O nanoparticles for gradual photo-reduction to Cu(0) nanoparticles. Furthermore, it has been reported in literature, TEOA cannot quench the excited state Fl*.[12,31] Therefore, when Fl is used as photosensitizer with TEOA as sacrificial electron donor in aqueous solution, the photochemical process is an oxidative quenching one: the electron transfers from Fl* to $Cu(OH)_2$ → Cu_2O (−0.08 V *vs.* NHE) and Cu_2O → Cu (−0.358 V *vs.* NHE).

Conclusions

In conclusion, we have successfully prepared Cu_2O and Cu nanoparticles from inorganic $CuSO_4$ precursor in alkaline aqueous solution in one photocatalytic system; while at the same time achieved efficient hydrogen evolution with *in situ* generated Cu nanoparticles. The photochemical process regarding the evolution of hydrogen and transformation from $Cu(OH)_2$ to Cu_2O to Cu was clarified based on XRD and induction period hydrogen evolution experiments. Cu_2O nanoparticles were obtained by photo-reduction of $CuSO_4$ (10^{-3} M) in TEOA solution after irradiation for 30 min, while Cu nanoparticles were obtained after 4 h of irradiation in both TEA and TEOA solutions. When the *in situ* prepared Cu_2O and Cu were isolated and re-added into the same photocatalytic system, the same photo-reduction process from Cu_2O to Cu photocatalyst was detected and the system was highly efficient for photocatalytic hydrogen production with TEOA as sacrificial regent. Single crystal of a $Cu(TEOA)(H_2O)_2$ complex and DLS experiments helped to reveal the presence of association and dissociation balance between decomposition of Cu^{2+} from TEOA and formation of $Cu(OH)_2$ in the alkaline solution. Our work was expected to provide some insight into utilization of solar energy for hydrogen evolution.

Conflicts of interest

There are no conflicts to declare.

Acknowledgements

This work was financially supported by the National Key Basic Research Program of China (973 Program 2013CB834804) and the Ministry of Science and Technology of China (2012DFH40090). W.-F. F. thanks the National Natural Science Foundation of China (21471155, 21777136) for financial support. C. J. Wang thanks the Incubation Program of Youth Innovation in Shandong Province for financial support.

References

1 G. W. Crabtree and N. S. Lewis, *Phys. Today*, 2007, **60**, 37–42.
2 D. G. Nocera, *ChemSusChem*, 2009, **2**, 387–390.
3 J. Xuan and W.-J. Xiao, *Angew. Chem., Int. Ed.*, 2012, **51**, 6828–6838.
4 D. G. Nocera, *Energy Environ. Sci.*, 2010, **3**, 993–995.
5 D. G. Nocera, *Inorg. Chem.*, 2009, **48**, 10001–10017.
6 T. S. Teets and D. G. Nocera, *Chem. Commun.*, 2011, **47**, 9268–9274.
7 P. Du and R. Eisenberg, *Energy Environ. Sci.*, 2012, **5**, 6012–6021.
8 W. T. Eckenhoff and R. Eisenberg, *Dalton Trans.*, 2012, **41**, 13004–13021.
9 A. J. Esswein and D. G. Nocera, *Chem. Rev.*, 2007, **107**, 4022–4047.
10 V. Artero, M. Chavarot-Kerlidou and M. Fontecave, *Angew. Chem., Int. Ed.*, 2011, **50**, 7238–7266.
11 W. Zhang, J. Hong, J. Zheng, Z. Huang, J. Zhou and R. Xu, *J. Am. Chem. Soc.*, 2011, **133**, 20680–20683.
12 Z. Han, W. R. McNamara, M.-S. Eum, P. L. Holland and R. Eisenberg, *Angew. Chem., Int. Ed.*, 2012, **51**, 1667–1670.
13 M. P. McLaughlin, T. M. McCormick, R. Eisenberg and P. L. Holland, *Chem. Commun.*, 2011, **47**, 7989–7991.
14 H.-Y. Wang, G. Si, W.-N. Cao, W.-G. Wang, Z.-J. Li, F. Wang, C.-H. Tung and L.-Z. Wu, *Chem. Commun.*, 2011, **47**, 8406–8409.
15 J. Han, W. Zhang, T. Zhou, X. Wang and R. Xu, *RSC Adv.*, 2012, **2**, 8293–8296.
16 W. R. McNamara, Z. Han, P. J. Alperin, W. W. Brennessel, P. L. Holland and R. Eisenberg, *J. Am. Chem. Soc.*, 2011, **133**, 15368–15371.
17 F. Lakadamyali, M. Kato, N. M. Muresan and E. Reisner, *Angew. Chem., Int. Ed.*, 2012, **51**, 9381–9384.
18 T. Yu, Y. Zeng, J. Chen, Y.-Y. Li, G. Yang and Y. Li, *Angew. Chem., Int. Ed.*, 2013, **52**, 5631–5635.
19 N. Wu, *Int. J. Hydrogen Energy*, 2004, **29**, 1601–1605.
20 W. J. Foo, C. Zhang and G. W. Ho, *Nanoscale*, 2013, **5**, 759–764.
21 I. Mondal, S. Gonuguntl and U. Pal, *J. Phys. Chem. C*, 2019, **123**(43), 26073–26081.
22 P. DeSario, J. Pietron, T. Brintlinger, M. McEntee, J. Parker, O. Baturina, R. Stroud and D. Rolison, *Nanoscale*, 2017, **9**, 11720–11729.
23 L. Tong, L. Ren, A. Fu, D. Wang, L. Liu and J. Ye, *Chem. Commun.*, 2019, **55**, 12900–12903.
24 Y. Yamada, T. Miyahigashi, H. Kotani, K. Ohkubo and S. Fukuzumi, *Energy Environ. Sci.*, 2012, **5**, 6111–6118.
25 C. N. R. Rao, H. S. S. Ramakrishna Matte, R. Voggu and A. Govindaraj, *Dalton Trans.*, 2012, **41**, 5089–5120.
26 F. Alonso, P. Riente, J. A. Sirvent and M. Yus, *Appl. Catal., A*, 2010, **378**, 42–51.
27 P.-Z. Li, A. Aijaz and Q. Xu, *Angew. Chem., Int. Ed.*, 2012, **51**, 6753–6756.
28 B. F. DiSalle and S. Bernhard, *J. Am. Chem. Soc.*, 2011, **133**, 11819–11821.
29 P. Jarosz, P. Du, J. Schneider, S.-H. Lee, D. McCamant and R. Eisenberg, *Inorg. Chem.*, 2009, **48**, 9653–9663.
30 C. J. Wang, S. Cao and W. F. Fu, *Chem. Commun.*, 2013, **49**, 11251–11253.

31 C. J. Wang, S. Cao, B. Qin, C. Zhang, T. T. Li and W. F. Fu, *ChemSusChem*, 2014, **7**, 1924–1933.
32 C. J. Wang, Y. Chen, X. J. Lv and W. F. Fu, *Appl. Catal., B*, 2016, **182**, 59–67.
33 K. Lalitha, G. Sadanandam, V. D. Kumari, M. Subrahmanyam, B. Sreedhar and N. Y. Hebalkar, *J. Phys. Chem. C*, 2010, **114**, 22181–22189.
34 J. Yu and J. Ran, *Energy Environ. Sci.*, 2011, **4**, 1364–1371.
35 F. Wen, X. Wang, L. Huang, G. Ma, J. Yang and C. Li, *ChemSusChem*, 2012, **5**, 849–853.
36 S. Min and G. Lu, *J. Phys. Chem. C*, 2011, **115**, 13938–13945.
37 Y. Liu, Y. Chu, Y. Zhuo, L. Dong, L. Li and M. Li, *Adv. Funct. Mater.*, 2007, **17**, 933–938.
38 S. B. Kalidindi, U. Sanyal and B. R. Jagirdar, *Phys. Chem. Chem. Phys.*, 2008, **10**, 5870–5874.
39 S. Min and G. Lu, *J. Phys. Chem. C*, 2011, **115**, 13938–13945.
40 T. Shimidzu, T. Iyoda and Y. Koide, *J. Am. Chem. Soc.*, 1985, **107**, 35–41.
41 X. Zhang, Z. Jin, Y. Li, S. Li and G. Lu, *J. Phys. Chem. C*, 2009, **113**, 2630–2635.
42 M. Zhou, M. Lin, Y. Wang, X. Guo, X. Guo, L. Peng and W. Ding, *Chem. Commun.*, 2011, **47**, 9268–9274.
43 M. Zhou, M. Li, C. Hou, Z. Li, Y. Wang, K. Xiang and X. Guo, *Chin. Chem. Lett.*, 2018, **29**, 787–790.
44 K. Koczkur, S. Mourdikoudis, L. Polavarapu and S. Skrabalak, *Dalton Trans.*, 2015, **44**, 17883–17905.
45 A. C. Brooks, K. Basore and S. Bernhard, *Inorg. Chem.*, 2013, **52**, 5794–5800.
46 J. Dong, M. Wang, X. Li, L. Chen, Y. He and L. Sun, *ChemSusChem*, 2012, **5**, 2133–2138.